Accurate Rigid-Body Modes Representation for a Nonlinear Curved Thin-Shell Element

T. Y. Yang*
Purdue University, West Lafayette, Indiana
Rakesh K. Kapania†
Virginia Polytechnic Institute and State University, Blacksburg, Virginia
and
Sunil Saigal‡
Worcester Polytechnic Institute, Worcester, Massachusetts

For certain highly curved shells, such as bellows, the formulation of a curved-shell finite element with curvilinear displacement components may fail to properly model some rigid body modes, even with either the explicit inclusion of rigid-body terms or the use of high-order displacement functions. It is suggested in this paper that the rigid-body modes can be properly included if the Cartesian displacement components are used. A 48-degree-of-freedom (DOF) curved thin-shell element is formulated, and both the curvilinear and the Cartesian forms are used for this investigation. Examples of the nonlinear analyses of a bellows shell and a spherical cap are given to demonstrate the advantage of using the Cartesian formulation. Curved elements may also suffer from membrane locking, which is caused by the inability of an element to bend without stretching. Numerical data are presented to show that the present element does not membrane lock. Some nonlinear examples are also presented to further demonstrate the versatility of this element.

Introduction

A PROBLEM that may prove to be of concern in the definition of displacement functions for curved thin-shell elements is the assurance of the presence of zero-strain energy modes of rigid-body displacement.[1] The use of high-order polynomials for curvilinear displacement functions may include the rigid-body modes implicitly[2-4] for a certain class of shells. Alternatively, curvilinear displacement functions may be used by including the rigid-body motion terms explicitly.[5,6] It has been pointed out,[7] however, that, for relatively large and highly curved shell elements, the former implicit formulation fails to properly include all the rigid-body modes, whereas the latter explicit formulation becomes too numerically sensitive and may yield a nonconvergent solution. Fonder and Clough[8] explicitly added four rigid-body modes in a cylindrical shell element with 24 DOF[9] and found significant improvement over the performance of the same element without this addition. However, after adding all six missing rigid-body modes to the doubly curved quadrilateral version of the same element, erroneous results were obtained. It was concluded that the addition of rigid-body modes is detrimental in shells of positive or negative Gaussian curvature. Also, a posteriori addition of rigid-body modes may render the elements incompatible along the curved boundaries of an element.

Isoparametric elements[10] provide another alternative for the analysis of shells. These elements avoid the use of a shell theory and provide for the inclusion of all rigid-body modes. However, a large number of DOF may result as several nodal points through the thickness have to be used. They also fail at a moderate length-to-thickness ratio due to shear locking.[11] Ahmad et al.[12] introduced the "degenerated" finite elements. The three-dimensional governing equations are discretized in terms of the variables on the midsurface for these elements. The constraint of straight normals is introduced, and the strain energy corresponding to the normal stresses is neglected. These elements allow for shear deformations, since the normals to the midsurface are not restricted to remain normal after deformation. This element and its numerous versions have been used for both linear and nonlinear applications.[13-19]

The degenerated thick-shell elements, when used to model thin shells, suffer from the phenomenon called shear locking. This phenomenon has been explained by, among others, Ramm,[13] Hughes et al.,[16] and Hughes and Liu.[17] In curved thin structures, such as arches and shells, where bending is predominant, the degenerated elements also suffer from membrane locking[20-22] when full orders of integration are used. These twin phenomena of shear and membrane locking may be overcome by the use of higher-order elements[20-22] or by resorting to reduced or selective integration as explained by, among others, Zienkiewicz and Hinton,[23] Pugh et al.,[24] Hughes et al.,[25] and Noor and Anderson.[26] Reference 23 provided a heuristic justification for reduced/selective integration on the basis of constraints. The use of higher-order elements leads to a large system of nonlinear equations. The use of reduced/selective integration leads to matrices that are rank deficient and possess spurious (or zero-energy) modes, known as the hourglass modes. Stabilization matrices are used to remove the spurious modes. The stabilization matrices were given by Jacquotte and Oden[27] for linear analysis and by Liu et al.[28] for nonlinear analysis. Hughes and Cohen[29] developed the "Heterosis" elements to obviate the problem of rank deficiency. Lee and Pian[30] developed a mixed formulation as a means for reducing the constraints of zero transverse shear strain energy when thick-plate elements are used for analyzing thin plates. It was shown that certain mixed formulations were equivalent to displacement formulations with a reduced integration scheme.

Received October 19, 1987; revision received May 17, 1988.

*Professor of Aeronautics and Astronautics and Dean of Engineering. Fellow AIAA.
†Assistant Professor, Department of Aerospace and Ocean Engineering. Member AIAA.
‡Assistant Professor, Mechanical Engineering Department. Associate Member AIAA.

It is noted that the rigid-body modes are correctly represented when flat-plate elements are used to model the shell structures.[11] This representation, however, has some major limitations. For example, the curved shell geometry is represented only approximately, and the flexural-membrane coupling within an element is not taken into account. Also, parasitic bending moments may occur due to this physical idealization. Some other difficulties associated with the flat-plate elements are singularity with coplanar elements, low-order membrane strain representation, displacement incompatibility, and inability to model imperfect and intersecting shells. A triangular faceted element, free from the problems faced by the existing flat-plate elements, was presented by Meek and Tan.[11]

The rigid-body displacement of a curved member is curvilinear and can be expressed as a function of trigonometric functions of the arc angle of the element.[1] If polynomial fields are used to define this curvilinear motion, the trigonometric functions will be reproduced only approximately. For a large arc angle of the element, the error in the approximation will increase. It follows then that, for an element formulated in the curvilinear field, the rigid-body modes will deteriorate when the element is used to model highly curved shells. In this study, it is shown that exact implicit modeling of the rigid-body modes for highly curved shell elements can be obtained by changing the displacement field from curvilinear to a Cartesian system.

Numerical results for a set of examples are presented using a 48-DOF curved finite element based on Cartesian displacements. The element is derived using the tensor formulation of geometrically nonlinear shell theory. The element seems to exhibit characteristics of a behavior free from both shear and membrane locking.

Finite-Element Formulations

The finite-element formulations are based on the Love-Kirchhoff thin-shell theory.[31,32] The geometry of the middle surface of the shell element is described by variable-order polynomials. The coefficients of these polynomials are based on the coordinates at given points on the middle surface of the element. Such a geometric representation allows the modeling of shell structures with quite an arbitrary distribution of curvatures.

Displacement Functions

The shell finite element is shown in Fig. 1. It has four nodes, one at each corner, and each node has 12 DOF. Two sets of nodal displacements have been investigated in this study: 1) curvilinear displacements and their derivatives with respect to curvilinear coordinates $u,u_\xi,u_\eta,u_{\xi\eta}$, and the same for v and w, and 2) Cartesian displacements and their derivatives with respect to curvilinear coordinates $\bar{u},\bar{u}_\xi,\bar{u}_\eta,\bar{u}_{\xi\eta}$, and the same for $\bar{v}$ and $\bar{w}$. The same interpolation functions are used for both the curvilinear and the Cartesian displacement functions, which are bicubic Hermitian polynomials in the curvilinear coordinates ξ and η.[2,3]

Strain-Displacement Relations

The shape of the shell is defined by the middle surface of the shell and the thickness h. The middle surface, which is smooth but otherwise of arbitrary shape, is defined by a vector r, which is given as

$$r = x^i e_i, \qquad i = 1,2,3 \tag{1}$$

where x^i is a fixed Cartesian coordinate system in three-dimensional space in which the middle surface is embedded, and e_i is a unit vector in x^i direction, as shown in Fig. 1.

The middle surface is also described by means of a system of parametric relations

$$x^i = f^i(\theta^1,\theta^2) \tag{2}$$

in which the parameters $\theta^\alpha(\alpha = 1,2)$ serve as coordinates on the surface and can be regarded as being an arbitrarily selected system. The two base vectors, a_1 and a_2 are obtained as derivatives of r with respect to each component θ^α, i.e.,

$$a_\alpha = r_{,\alpha} = \frac{\partial f^i}{\partial \theta^\alpha} e_i = f^i_{,\alpha} e_i \tag{3}$$

The unit normal to the surface a_3 is given as

$$a_3 = (a_1 \times a_2)/|a_1 \times a_2| = n^i e_i \tag{4}$$

where

$$n^i = c e_{ijk} f^j_{,1} f^k_{,2} \tag{5}$$

where e_{ijk} is the alternating symbol

$$c = [|a_1 \times a_2|]^{-1} = 1/\sqrt{a} \tag{6}$$

$$a = \begin{vmatrix} a_{11} & a_{12} \\ a_{21} & a_{22} \end{vmatrix} \tag{7}$$

$$a_{\alpha\beta} = a_\alpha \cdot a_\beta = f^i_{,\alpha} f^i_{,\beta} \tag{8}$$

$a_{\alpha\beta}$ is the metric tensor and yields the first fundamental form of a surface

$$ds^2 = a_{\alpha\beta}\, d\theta^\alpha\, d\theta^\beta \tag{9}$$

where ds is the distance between two neighboring points at θ^α, and $\theta^\alpha + d\theta^\alpha(\alpha = 1,2)$. Similarly, the second fundamental tensor or the curvature tensor of the surface $b_{\alpha\beta}$ is given as[32]

$$b_{\alpha\beta} = n^i \frac{\partial^2 f^i}{\partial\theta^\alpha \partial\theta^\beta} = n^i f^i_{,\alpha\beta} \tag{10}$$

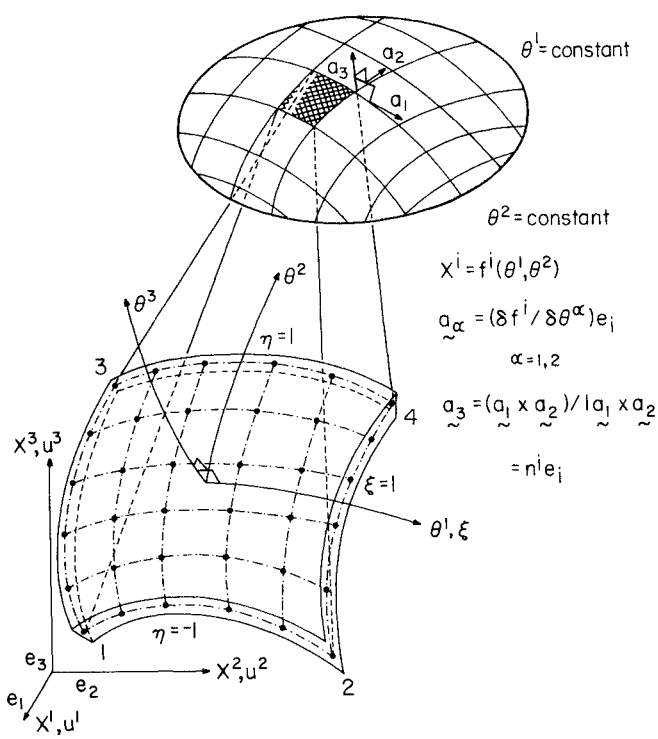

Fig. 1 A curved quadrilateral 48-DOF thin-shell finite element.

A point on the middle surface with the coordinates θ^α has the Cartesian coordinates $f^i(\theta^1,\theta^2)$ in the initial state. After deformation, the same point has the Cartesian coordinates $f^i + u^i$, where u^i are the Cartesian components of the displacement vector and give complete information about the deformation of the middle surface.

In the deformed state, the fundamental and the curvature tensors take the form $\bar{a}_{\alpha\beta}$ and $\bar{b}_{\alpha\beta}$, respectively:

$$\bar{a}_{\alpha\beta} = (f^i + u^i)_{,\alpha}(f^i + u^i)_{,\beta} = \bar{f}^i_{,\alpha}\bar{f}^i_{,\beta} \tag{11}$$

$$\bar{b}_{\alpha\beta} = \bar{n}^i \bar{f}^i_{,\alpha\beta} \tag{12}$$

where

$$\bar{n}^i = (\bar{a})^{-1/2} e_{ijk}\, \bar{f}^j_{,1}\bar{f}^k_{,2} \tag{13}$$

The value of $(\bar{a})^{-1/2}$ can be approximated as

$$(\bar{a})^{-1/2} = (a)^{-1/2}[1 - (A/a)]$$

where

$$A = (\epsilon_{11}a_{22} + \epsilon_{22}a_{11} - 2\epsilon_{12}a_{12}) \tag{14}$$

In Eq. (14), $\epsilon_{\alpha\beta}$ are the tangential strain measures and are given as

$$\epsilon_{\alpha\beta} = \tfrac{1}{2}(\bar{a}_{\alpha\beta} - a_{\alpha\beta}) = \tfrac{1}{2}(f^i_{,\alpha}u^i_{,\beta} + u^i_{,\alpha}f^i_{,\beta} + u^i_{,\alpha}u^i_{,\beta}) \qquad i = 1,2,3 \tag{15}$$

The terms $u^i_{,\alpha}u^i_{,\beta}$ are the nonlinear terms which are neglected in linear analysis but retained in the present study.

The curvature measure is given as[32]

$$k_{\alpha\beta} = -(\bar{b}_{\alpha\beta} - b_{\alpha\beta}) + \tfrac{1}{2}(b^\delta_\alpha \epsilon_{\beta\delta} + b^\delta_\beta \epsilon_{\alpha\delta}) \tag{16}$$

It can be proved, by substituting expressions for $\bar{b}_{\alpha\beta}$ from Eqs. (12–14) in Eq. (16), that

$$\begin{aligned} k_{\alpha\beta} = & -\{[(f^2_{,2}f^3_{,\alpha\beta} - f^3_{,2}f^2_{,\alpha\beta}) - A_1 S_{,\alpha\beta}]u^1_{,1} \\ & + [(f^3_{,1}f^2_{,\alpha\beta} - f^2_{,1}f^3_{,\alpha\beta}) - B_1 S_{,\alpha\beta}]u^1_{,2} \\ & + [(f^3_{,2}f^1_{,\alpha\beta} - f^1_{,2}f^3_{,\alpha\beta}) - A_2 S_{,\alpha\beta}]u^2_{,1} \\ & + [(f^1_{,1}f^3_{,\alpha\beta} - f^3_{,1}f^1_{,\alpha\beta}) - B_2 S_{,\alpha\beta}]u^2_{,2} \\ & + [(-f^2_{,2}f^1_{,\alpha\beta} + f^1_{,2}f^2_{,\alpha\beta}) - A_3 S_{,\alpha\beta}]u^3_{,1} \\ & + [(f^2_{,1}f^1_{,\alpha\beta} - f^1_{,1}f^2_{,\alpha\beta}) - B_3 S_{,\alpha\beta}]u^3_{,2} \\ & + (f^2_{,1}f^3_{,2} - f^3_{,1}f^2_{,2})u^1_{,\alpha\beta} + (f^3_{,1}f^1_{,2} - f^1_{,1}f^3_{,2})u^2_{,\alpha\beta} \\ & + (f^1_{,1}f^2_{,2} - f^2_{,1}f^1_{,2})u^3_{,\alpha\beta}\}\,(a)^{-1/2} + \tfrac{1}{2}(b^\delta_\alpha \epsilon_{\beta\delta} + b^\delta_\beta \epsilon_{\alpha\delta}) \end{aligned} \tag{17}$$

In Eq. (17),

$$\begin{aligned} A_i &= f^i_{,1}a_{22} - f^i_{,2}a_{12} \\ B_i &= f^i_{,2}a_{11} - f^i_{,1}a_{12} \\ S_{\alpha\beta} &= (1/a)\, e_{ijk}\, f^i_{,\alpha\beta} f^j_{,1} f^k_{,2} \end{aligned} \tag{18}$$

In deriving the curvature term in Eq. (17), the nonlinear terms were neglected. It should be noted that the linear curvature tensor is valid for problems with moderate bending.[33] A linear curvature tensor is common in several finite-element formulations (see, for example, Refs. 34–36) and several large displacement shell theories. A review of the different nonlinear theories containing different combinations of quadratic and cubic terms in curvature tensor was given by Nolte et al.[37] The results for a highly nonlinear example (a hemispherical shell under ring load) were presented. It was shown that, for problems with large rotations, higher-order terms in curvature are important and thus must be taken into account.

Stress-Strain Relations

In the elastic range, the constitutive equations can be given as

$$N^{\alpha\beta} = H^{\alpha\beta\lambda\mu} e_{\lambda\mu} \tag{19}$$

$$M^{\alpha\beta} = (h^2/12) H^{\alpha\beta\lambda\mu} k_{\lambda\mu} \tag{20}$$

$N^{\alpha\beta}$ and $M^{\alpha\beta}$ are the in-plane stress resultant tensor and the stress couple tensor, respectively; $e_{\lambda\mu}$ and $k_{\lambda\mu}$ are the tangential strain tensor and the curvature tensor, respectively; and $H^{\alpha\beta\lambda\mu}$ is the tensor of elastic moduli. Equations (19) and (20) can be written in matrix form as

$$\{\Sigma\} = \begin{Bmatrix} N \\ M \end{Bmatrix} = \begin{bmatrix} D^e_m & 0 \\ 0 & D^e_b \end{bmatrix} \begin{Bmatrix} e \\ k \end{Bmatrix} = [D^e][E] \tag{21}$$

where $D^e_b = (h^2/12)D^e_m$. All strains and stresses are defined in the tensor form as given in Eqs. (19) and (20). When determining the plastic zones, the strains and stresses must be converted from tensor form to vector form as

$$\sigma^{\alpha\beta} = a_{\alpha\beta} N^{\alpha\beta} \tag{22}$$

$$\epsilon^{\alpha\beta} = a_{\alpha\beta} e^{\alpha\beta} \tag{23}$$

so that their physical quantities can be identified.

The stress-strain relations in the plastic range are finally obtained in a matrix form as

$$\{\Sigma\} = \begin{Bmatrix} N \\ M \end{Bmatrix} = \begin{bmatrix} D^p_m & 0 \\ 0 & D^p_b \end{bmatrix} \begin{Bmatrix} e \\ k \end{Bmatrix} = [D^p]\{E\} \tag{24}$$

where

$$[D^p_m] = [D^e_m] - \frac{[D^e_m]\{a\}\{a\}^T[D^e_m]}{A + \{a\}^T[D^e_m]\{a\}} \tag{25}$$

where $\{a\}$ is the flow vector, and A is hardening function. The preceding notations follow those of Refs. 38 and 39.

Solution Procedure

In this study, the incremental solution procedure was used. Only a brief description of the derivation of the tangent stiffness matrix is given. A detailed description of the derivation of the incremental equation of motion can be found in, for example, Ref. 38. Since the total Lagrangian formulation is used, all field quantities of shell deformations are referred to the known undeformed shell middle surface. Let $\bar{u}$ be the displacement vector of a material point in the undeformed shell middle surface to its position in the deformed configuration. Let $\hat{u}$ be the incremental displacement vector of the same point.

Referring to the undeformed middle surface, the displacement field of the final configuration can be expressed as

$$u = \bar{u} + \hat{u} \tag{26}$$

The middle-surface strain tensor $\epsilon_{\alpha\beta}$ and the curvature tensor $k_{\alpha\beta}$ are in the following form:

$$\epsilon_{\alpha\beta} = \bar{\epsilon}_{\alpha\beta} + \hat{\epsilon}_{\alpha\beta} \tag{27}$$

$$k_{\alpha\beta} = \bar{k}_{\alpha\beta} + \hat{k}_{\alpha\beta} \tag{28}$$

where $\bar{\epsilon}_{\alpha\beta}$ is obtained by substituting $\bar{u}$ in Eq. (15). Similarly, $\bar{k}_{\alpha\beta}$ and $\hat{k}_{\alpha\beta}$ can be obtained by substituting $\bar{u}$ and $\hat{u}$, respectively, in Eq. (17).

Because of the presence of nonlinear terms in Eq. (15), $\hat{\epsilon}_{\alpha\beta}$ cannot be obtained by merely substituting $\hat{u}$ in Eq. (15). It is a function of both $\bar{u}$ and $\hat{u}$.

It can be shown that the incremental strain tensor is given as

$$\hat{\epsilon}_{\alpha\beta} = \epsilon_{\alpha\beta}(u) - \epsilon_{\alpha\beta}(\bar{u})$$
$$= \tfrac{1}{2}(f^i_{,\alpha}\hat{u}^i_{,\beta} + f^i_{,\beta}\hat{u}^i_{,\alpha} + \hat{u}^i_{,\alpha}\hat{u}^i_{,\beta} + \bar{u}^i_{,\alpha}\hat{u}^i_{,\beta} + \bar{u}^i_{,\beta}\hat{u}^i_{,\alpha}) \quad (29)$$

From Eqs. (17) and (29), we can write the expression for incremental strain and curvature as

$$\{d\epsilon\} = \begin{Bmatrix} \hat{\epsilon}_{\alpha\beta} \\ \hat{k}_{\alpha\beta} \end{Bmatrix} = [A_0 + A_L(\bar{u})]\{\hat{u}\} \quad (30)$$

where $[A_0]$ is the same matrix as in linear infinitesimal strain analysis, and $[A_L]$ depends upon the displacements.

The three components of the incremental displacement vector are related to the element DOF $\{\hat{q}_e\}$ through the element shape functions $[N]$ as

$$\{\hat{u}\} = [N]\{\hat{q}_e\} \quad (31)$$

Substituting Eq. (31) in Eq. (30), we get

$$\{d\epsilon\} = [B_0 + B_L(q_e)]\{\hat{q}_e\} \quad (32)$$

Following a procedure similar to one outlined in Ref. 38, we obtain

$$[K_T]\{\hat{q}_e\} = \{\hat{p}_e\} \quad (33)$$

where $[K_T]$ is the tangent stiffness matrix, $\{\hat{q}_e\}$ is the incremental displacement vector and $\{\hat{p}_e\}$ is the vector of unbalanced forces.

The tangent stiffness matrix is given as

$$[K_T] = \iint_A [B_0 + B_L(q_e)]^T[D][B_0 + B_L(q_e)]\sqrt{a}\, d\theta^1\, d\theta^2 + \iint_A [G]^T[H][G]\sqrt{a}\, d\theta^1\, d\theta^2 \quad (34)$$

In Eq. (34), $[D]$ is the stress-strain matrix, as described in an earlier section. The second integral yields the incremental stiffness matrix.

The matrix $[G]$ is given by

$$[\hat{u}^1_{,1}\hat{u}^2_{,1}\hat{u}^3_{,1}\hat{u}^1_{,2}\hat{u}^2_{,2}\hat{u}^3_{,2}] = [G]\{\hat{q}_e\} \quad (35)$$

The matrix $[H]$ is given as

$$[H] = \begin{bmatrix} H_{11} & H_{12} \\ H_{21} & H_{22} \end{bmatrix} \qquad H_{\alpha\beta} = N^{\alpha\beta}\begin{bmatrix} 1 & 0 & 0 \\ 0 & 1 & 0 \\ 0 & 0 & 1 \end{bmatrix} \quad (36)$$

The incremental load vector $\{\hat{p}_e\}$ is given as

$$\{\hat{p}_e\} = \{p_e\} - \iint_A [B_0 + B_L(q)]^T \begin{Bmatrix} N^{\alpha\beta}(q) \\ M^{\alpha\beta}(q) \end{Bmatrix} \sqrt{a}\, d\theta^1\, d\theta^2 \quad (37)$$

where $\{p_e\}$ is the total applied load vector, and the second term yields the total internal load vector.

The element matrices given in Eq. (33) can be assembled to yield

$$[K_T]\{\hat{q}\} = [\hat{P}] \quad (38)$$

The tangent stiffness matrix $[K_T]$ may or may not be updated in every iteration cycle. In each step, iterations were continued until the norm of incremental displacements and forces were within 0.1% of the norms of total displacements and forces, respectively.

Numerical Results

To evaluate the present formulations, a variety of shell problems is chosen to study the phenomenon of membrane locking and the comparison between Cartesian and curvilinear displacement formulations. The results of linear static analysis of a pinched cylindrical shell and a point-loaded hemispherical shell are given first. Membrane locking in both these shells can be pronounced.[21] Nonlinear analyses of a semitoroidal bellows and a hinged spherical cap are then performed using both the curvilinear and the Cartesian formulations for each analysis. The advantage of the Cartesian formulation is shown by comparing the results with existing alternative solutions. The results for snap-back of a cylindrical panel are presented to demonstrate the versatility of the present element.

Hemispherical Shell Under External Pressure

Bushnell[40] suggested the problem of a free hemispherical shell pinched by a $\cos 2\theta$ pressure distribution as a test case to evaluate the performance of a given finite element. The problem is ill-conditioned, since small forces cause large displacements. The geometric data for the problem are shown in Fig. 2. The material data are given as $E = 10^7$ psi, and $\nu = 0.3$.

In this study, six different meshes ($M \times N = 1 \times 1$, 2×1, 4×2, 6×2, 6×3, and 8×3) were used to model a quarter of

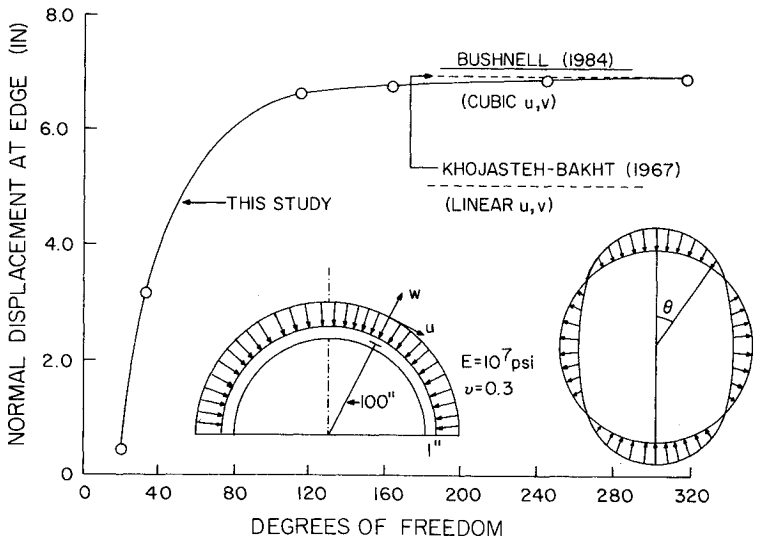

Fig. 2 Convergence study for the 48-DOF thin-shell finite element. Hemispherical shell under external pressure.

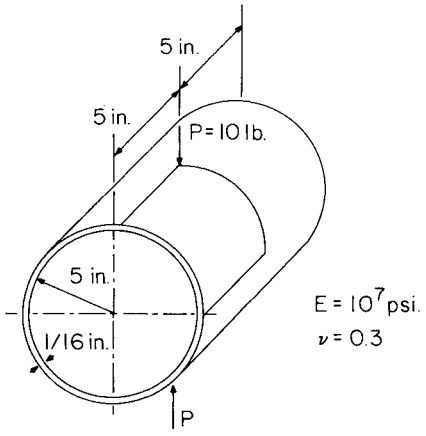

Fig. 3 A pinched cylindrical shell.

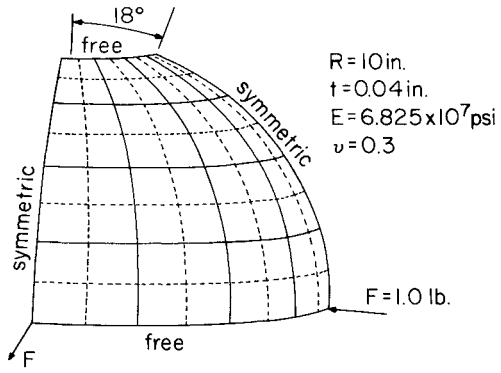

Fig. 4 A point-loaded spherical shell.

the hemisphere, where M is defined as the number of elements in the meridional direction and N as the number of elements in the circumferential direction. The present results for maximum normal deflection at the free edge at $\theta = 0$ vs mesh refinement are shown in Fig. 2, with only the converged values obtained using the energy finite-difference method[41] and the finite-element method using linear u and v and cubic w, and cubic u, v, and w.[40] A good agreement of results was obtained.

Linear Analysis of a Pinched Cylindrical Shell

The cylinder shown in Fig. 3 was analyzed with a pair of diametrically pinched loads of 10 lb each. Because of double symmetry of the shell, only an octant was modeled, and five different meshes were used: 1×1, 2×1, 3×1, 4×1, and 5×1, with the number of elements increasing in the circumferential direction. The results were obtained for three different orders of full integration for each mesh: 3×3, 4×4, and 5×5. The results are shown in Table 1. The results appear to be independent of the higher orders of quadrature, indicating that the element does not suffer from membrane locking.

Linear Analysis of Hemispherical Shell Subjected to Concentrated Forces

Figure 4 shows an octant of a hemispherical shell subjected to two equal and opposite loads. The octant is modeled using four different meshes: 2×2, 4×4, 6×6, and 8×8. Results were obtained using three different orders of full integration: 3×3, 4×4, and 5×5. The results are shown in Table 2. Again, the fact that the results do not deteriorate with an increase in the order of integration indicates that the element does not suffer from membrane locking.

Table 1 Radial displacement under load for a pinched cylinder

Mesh size	Radial displacement, in. 3×3 integration	4×4 integration	5×5 integration
1×1	0.4052×10^{-1}	0.4384×10^{-3}	0.4384×10^{-3}
2×1	0.3199×10^{-1}	0.2905×10^{-1}	0.2819×10^{-1}
3×1	0.3934×10^{-1}	0.3805×10^{-1}	0.3805×10^{-1}
4×1	0.4175×10^{-1}	0.4121×10^{-1}	0.4121×10^{-1}
5×1	0.4251×10^{-1}	0.4229×10^{-1}	0.4229×10^{-1}

Table 2 Radial displacement under load for a point loaded spherical shell

Mesh size	Radial displacement, in. 3×3 integration	4×4 (also 5×5) integration
2×2	0.3029×10^{-1}	0.1461×10^{-1}
4×4	0.8269×10^{-1}	0.7802×10^{-1}
6×6	0.9091×10^{-1}	0.8988×10^{-1}
8×8	0.9262×10^{-1}	0.9215×10^{-1}

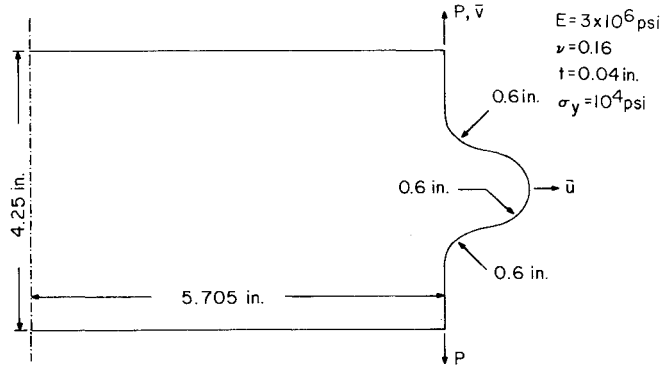

Fig. 5 An axisymmetric semitoroidal bellows.

Semitoroidal Bellows Under Axisymmetric Load into the Plastic Range

The axisymmetric semitoroidal bellows shown in Fig. 5 was studied next. This structure has previously been analyzed by Zienkiewicz and Nayak[42] and Surana[43] using axisymmetric finite elements. The bellows is characteristic in that it has regions of positive, negative, and zero Gaussian curvature. This shell was assumed to be loaded to $P = 600$ lb with plastic deformations. Convergence study was made, and the effect of rigid-body modes due to Cartesian displacement formulation was observed.

The bellows was first analyzed using the curvilinear displacement formulations. The percentage errors in displacements were plotted against the increasing number of elements in Fig. 6 using dotted lines. The results fail to converge to the correct answer as the number of elements is sufficiently increased. An investigation of the eigensolutions of each of the elements used to model the bellows revealed that the rigid-body motions along the axial directions were not modeled properly in the region with nonzero Gaussian curvature. Improper rigid-body motions can induce strains of significant magnitude with respect to real straining modes, leading to erroneous results.

The bellows was then analyzed using the Cartesian displacement formulation. The results for percentage errors in displacements with increasing number of elements were also plotted in Fig. 6 using solid lines. It is seen that the results

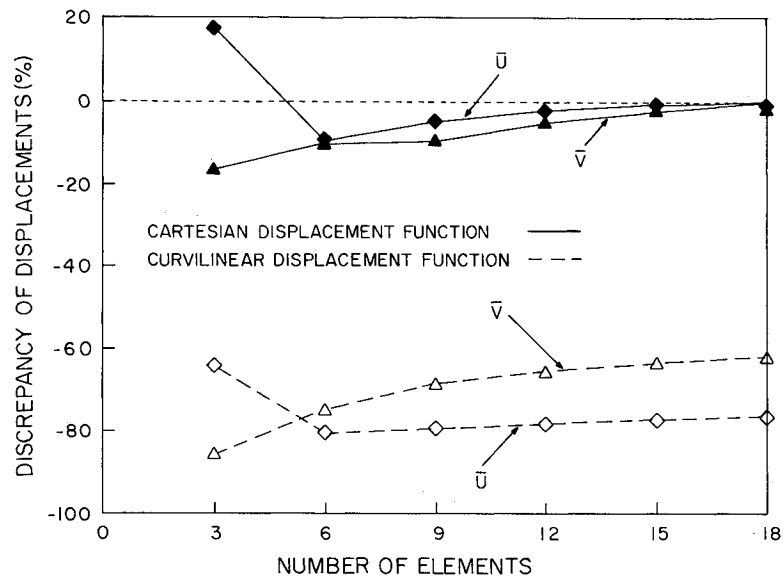

Fig. 6 Convergence study for curvilinear and Cartesian formulations of 48-DOF shell element for the elastic/perfectly plastic semitoroidal bellows under load P = 600 lb.

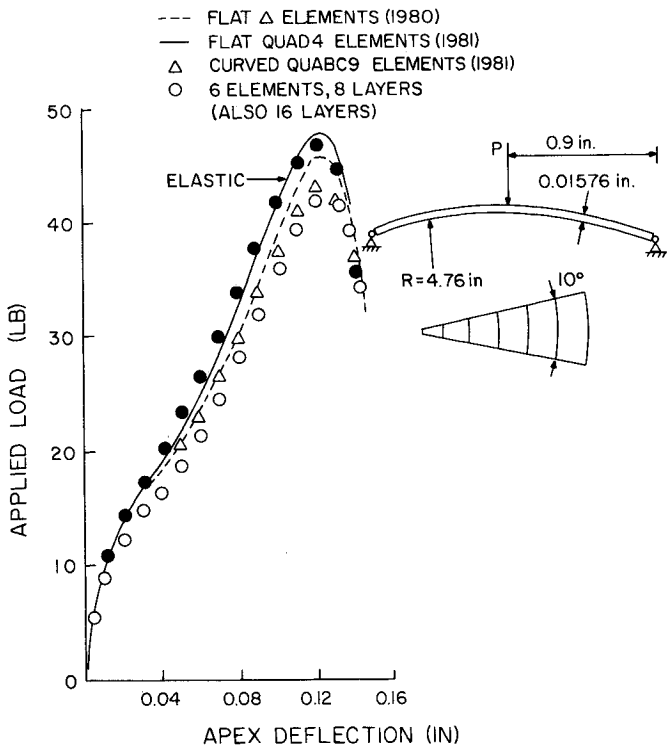

Fig. 7 Load-displacement curve for a hinged spherical cap under apex load.

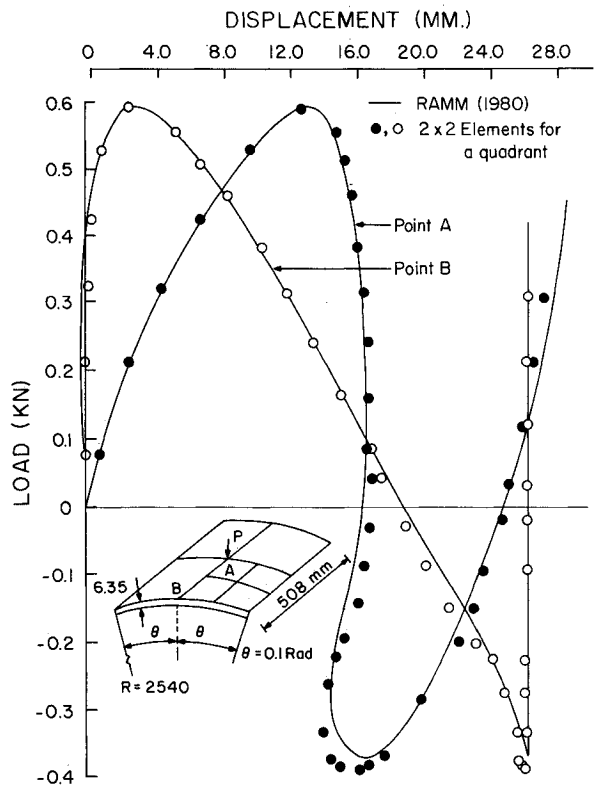

Fig. 8 Load-deflection curve for a hinged cylindrical panel.

converge quickly. This quick convergence of displacements due to Cartesian displacement formulation was shown in Ref. 44 for the elastic case. The present elastic-plastic example further demonstrates the advantage of using Cartesian displacement formulation.

Nonlinear Analysis of a Hinged Spherical Cap Under Apex Load

A spherical cap loaded at the apex and supported on a fixed hinge at the circumference was considered. The material properties of the cap are $E = 10^7$ psi, $\nu = 0.3$. This problem has previously been considered by Argyris et al.[45] using flat-plate elements and by Parisch[46] using flat QUAD4 elements and curved shell elements QUABC9.

The cap was analyzed using the present 48-DOF element. Because of axisymmetry, only a 10-deg segment of the cap was modeled and six elements were used. The results were obtained for both the curvilinear and the Cartesian displacement formulations. The solutions for both cases were plotted in Fig. 7. Because of the softening behavior of the spherical cap, this nonlinear analysis was done using a displacement-increment procedure instead of a load-increment procedure.

It is seen that the results obtained using both versions of the present element are in agreement with the previous results. Both the flat-plate elements and the present 48-DOF element with Cartesian formulations accurately include the rigid-body modes. The stiffer results are believed to be more accurate than those obtained by using the curvilinear formulations, which may be in error due to improper modeling of the rigid-body modes. The capability to accurately include rigid-body modes seems essential if the element has to be used for problems that entail large displacements.[47]

Shallow Cylindrical Shell Under Point Load

The element formulated in the Cartesian coordinates is used to study the geometrically nonlinear behavior of a shallow cylindrical shell under a concentrated load. The shell shown in Fig. 8 is hinged at the longitudinal edges and is free along the curved boundaries. The material properties are $E = 3.101$ kN/mm^2 and $v = 0.3$. The structure exhibits snap-through as well as snap-back phenomena, with horizontal and vertical tangents. The shell was analyzed by Sabir and Lock,[48] who used a combination of displacement- and load-control techniques. This problem was also analyzed by Ramm,[49] using bicubic degenerated shell elements. Since the shell exhibits snap-back phenomenon, the displacement increment procedure cannot be used to obtain the load-displacement path. Various other methods have been proposed to overcome this difficulty. These include, among others, suppression of iterations near limit points, the constant-arc methods of Wempner[50] and Riks,[51] and the current stiffness parameter method.[52] The method of Wempner and Riks was employed here to study the cylindrical shell. It may be noted that, in its original form, the Riks-Wempner method renders the system of equations to be nonsymmetric and unbanded. To overcome this limitation, a modified version of this method, based on the displacement increment method of Batoz and Dhatt,[53] was suggested by Ramm.[49]

Because of symmetry, only a quarter of the shell was modeled using a 2×2 mesh. An initial load step of 0.2 kN was chosen, and the load steps were adjusted at each step by relating the number of iterations n_i used in the previous step to a desired value n_d. Ramm[49] suggested the use of factor $\sqrt{n_d/n_i}$ to scale the previous load step. A value of $n_d = 7$ was used in this study. Such a scaling is especially useful in the vicinity of the point of minimum load. This portion of the load-displacement path is difficult due to an abrupt change of response, for instance, here at point B.

The results were plotted in Fig. 8 for the load vs displacement behavior at points A and B on the cylindrical shell. The results are in good agreement with earlier results.

Concluding Remarks

The accurate representation of the rigid-body modes is achieved for a 48-DOF arbitrarily curved, but not skewed, thin-shell finite element by formulation using displacement functions to interpolate the Cartesian displacement components instead of the curvilinear displacement components. The linear and nonlinear behaviors predicted by using the curvilinear formulation may converge to the wrong solution due to an appreciable straining caused by the zero-strain rigid-body motions compared to the real straining modes. This effect may be especially pronounced for a certain class of highly curved shells and shells with negative Gaussian curvature.

A curved-shell element is presented in this study which does not suffer from the phenomenon of "membrane locking" which is common in many curved elements. This may be due to the use of the same high order for polynomials to describe the inplane displacements as the normal displacement. A highly nonlinear shell problem with snap-through and snap-back has been presented to demonstrate further the versatility of this element.

Acknowledgment

The authors acknowledge the National Science Foundation for Research Grant MSM-8313360. They acknowledge D. K. Liaw for obtaining data for the convergence study in Fig. 6, and T. B. Belytschko for his valuable comments through correspondence in 1985.

References

[1]Gallagher, R. H., "Problems and Progress in Thin Shell Finite Element Analysis," *Finite Elements for Thin Shells and Curved Members,* edited by D. G. Ashwell and R. H. Gallagher, Wiley, New York, 1976, pp. 1-14.

[2]Bogner, F. K., Fox, R. L., and Schmit, L. A., Jr., "A Curved Cylindrical-Shell Finite Element," *AIAA Journal,* Vol. 5, April 1967, pp. 745-750.

[3]Mebane, P. and Stricklin, J., "Implicit Rigid Body Motion in Curved Finite Elements," *AIAA Journal,* Vol. 9, Feb. 1971, pp. 344-345.

[4]Yang, T. Y., "High Order Rectangular Shallow Shell Finite Element," *Journal of the Engineering Mechanics Division, ASCE,* Vol. 99, No. EM1, 1973, pp. 157-181.

[5]Cantin, G. and Clough, R. W., "A Curved Cylindrical-Shell Finite Element," *AIAA Journal,* Vol. 6, June 1968, pp. 1057-1062.

[6]Cantin, G., "Rigid Body Motions in Curved Finite Elements," *AIAA Journal,* Vol. 8, July 1970, pp. 1252-1255.

[7]Fonder, G. A., "Studies in Doubly-Curved Elements for Shells of Revolution," *Finite Elements for Thin Shells and Curved Members,* edited by D. G. Ashwell and R. H. Gallagher, Wiley, New York, 1976, pp. 113-130.

[8]Fonder, G. A. and Clough, R. W., "Explicit Addition of Rigid-Body Motions in Curved Finite Elements," *AIAA Journal,* Vol. 11, March 1973, pp. 305-312.

[9]Gallagher, R. H., "The Development and Evaluation of Matrix Methods for Thin Shell Structural Analysis," Ph.D. Thesis, State Univ. of New York, Buffalo, NY, 1964.

[10]Ergatoudis, J., Irons, B. M., and Zienkiewicz, O. C., "Curved Isoparametric Quadrilateral Elements for Finite Element Analysis," *International Journal of Solids and Structures,* Vol. 4, Jan. 1968, pp. 31-42.

[11]Meek, J. L. and Tan, H. S., "A Faceted Shell Element with Loof Nodes," *International Journal for Numerical Methods in Engineering,* Vol. 23, Jan. 1986, pp. 49-67.

[12]Ahmad, S., Irons, B. M., and Zienkiewicz, O. C., "Curved Isoparametric Quadrilateral Elements for Finite Element Analysis," *International Journal for Numerical Methods in Engineering,* Vol. 2, Feb. 1970, pp. 419-451.

[13]Ramm, E., "A Plate/Shell Element for Large Deflections and Rotations," *Formulations and Computational Algorithms in Finite Element Analysis: U.S.-Germany Symposium,* edited by K. J. Bathe, J. T. Oden, and W. Wunderlich, MIT Press, Cambridge, MA, 1977, Chap. 10, pp. 264-293.

[14]Parisch, H., "Geometric Nonlinear Analysis of Shells," *Computer Methods in Applied Mechanics and Engineering,* Vol. 14, Feb. 1978, pp. 159-178.

[15]McNeal, R. H., "A Simple and Quadrilateral Shell Element," *Computers and Structures,* Vol. 8, No. 2, April 1978, pp. 175-183.

[16]Hughes, T. J. R., Taylor, R. L., and Kanoknukulchai, A., "A Simple and Efficient Element for Plate Bending," *International Journal for Numerical Methods in Engineering,* Vol. 11, Oct. 1977, pp. 1529-1543.

[17]Hughes, T. J. R. and Liu, W. K., "Nonlinear Finite Element Analysis of Shells: Part I. Three Dimensional Shells," *Computer Methods in Applied Mechanics and Engineering,* Vol. 26, March 1981, pp. 331-362.

[18]Ramm, E. and Stegmuller, H., "The Displacement Finite Element Method in Nonlinear Buckling Analysis," *Buckling of Shells,* edited by E. Ramm, Springer-Verlag, Berlin, 1982, pp. 201-235.

[19]Milford, R. V. and Schnobrich, W. C., "Degenerated Isoparametric Finite Elements Using Explicit Integration," *International Journal for Numerical Methods in Engineering,* Vol. 23, Jan. 1986, pp. 133-154.

[20]Stolarski, H. and Belytschko, T., "Membrane Locking and Reduced Integration for Curved Elements," *Journal of Applied Mechanics,* Vol. 49, No. 1, March 1982, pp. 172-176.

[21]Stolarski, H. and Belytschko, T., "Shear and Membrane Locking in Curved C° Elements," *Computational Methods in Applied Mechanics and Engineering,* Vol. 41, No. 3, Dec. 1983, pp. 279-296.

[22]Belytschko, T., Liu, W.-K., Ong, J. S.-J., and Lam, D., "Implementation and Application of a 9-Node Lagrange Shell Element with Spurious Mode Control," *Computers and Structures,* Vol. 20, No. 1-3, 1985, pp. 121-128.

[23]Zienkiewicz, O. C. and Hinton, E., "Reduced Integration, Function Smoothing and Nonconformity in Finite Element Analysis (with Special Reference to Thick Plates)," *Journal of the Franklin Institute,* Vol. 302, Nov./Dec. 1976, pp. 443-461.

[24]Pugh, E. D. L., Hinton, E., and Zienkiewicz, O. C., "A Study of Quadrilateral Plate Bending Elements with Reduced Integration," *International Journal for Numerical Methods in Engineering,* Vol. 12, July 1978, pp. 1059-1079.

[25]Hughes, T. J. R., Cohen, M., and Haroun, M., "Reduced and Selective Integration Techniques in the Finite Element Analysis of Plates," *Nuclear Engineering and Design,* Vol. 46, No. 1, March 1978, pp. 445–450.

[26]Noor, A. K. and Anderson, C. M., "Mixed Models and Reduced/Selective Integration Displacement Models for Nonlinear Shell Analysis," *Nonlinear Finite Element Analysis,* edited by T. J. R. Hughes, A. Pifko, and A. Jay, Proceedings of the ASME Winter Annual Meeting, AMD-Vol. 48, 1981.

[27]Jacquotte, O. P. and Oden, J. T., "Analysis and Treatment of Hourglass Instabilities in Underintegrated Finite Element Methods," *Proceedings of the International Conference on Innovative Methods for Nonlinear Analysis,* edited by W. K. Liu, T. Belytschko, and K. C. Park, 1984, Pineridge Press International Ltd., Swansea, Wales, UK, 1984, pp. 259–268.

[28]Liu, W. K., Belytschko, T., and Ong, J. S.-J., "The Use of Stabilization Matrices in Nonlinear Analysis," *Proceedings of the International Conference on Innovative Methods for Nonlinear Problems,* edited by W. K. Liu, T. Belytschko, and K. C. Park, Pineridge Press International Ltd., Swansea, Wales, UK, 1984, pp. 233–258.

[29]Hughes, T. J. R. and Cohen, M., "The 'Heterosis' Finite Element for Plate Bending," *Computers and Structures,* Vol. 9, No. 5, Nov. 1978, pp. 445–450.

[30]Lee, S. W. and Pian, T. H. H., "Improvement of Plate and Shell Finite Elements by Mixed Formulations," *AIAA Journal,* Vol. 16, Jan. 1978, pp. 29–34.

[31]Novozhilov, V. V., *Foundations of Nonlinear Theory of Elasticity,* Graylock Press, Rochester, NY, 1953.

[32]Niordson, F. I., *Introduction to Shell Theory,* Solid Mechanics, Technical Univ. of Denmark, Lyngby, Denmark, 1980.

[33]Mushtari, K. and Galimov, K., "Nonlinear Theory of Elastic Shells," NASA TT-F62, 1962.

[34]Bergan, P. G. and Clough, R. W., "Large Deflection Analysis of Plates and Shallow Shells Using the Finite Element Method," *International Journal for Numerical Methods in Engineering,* Vol. 5, March 1973, pp. 543–556.

[35]Thomas, G. R. and Gallagher, R. H., "A Triangular Thin Shell Finite Element: Nonlinear Analysis," NASA CR-2483, 1975.

[36]Pica, A. and Wood, R. D., "Postbuckling Behavior of Plates and Shells Using a Mindlin Shallow Shell Formulation," *Computers and Structures,* Vol. 12, No. 5, Nov. 1980, pp. 759–768.

[37]Nolte, L.-P., Makowski, J., and Stumf, H., "On the Derivation and Comparative Analysis of Large Rotation Shell Theories," *Ingenieur-Archiv,* Vol. 56, Feb. 1986, pp. 145–160.

[38]Zienkiewicz, O. C., *The Finite Element Method,* 3rd ed., McGraw-Hill, London, England, UK, 1977.

[39]Yang, T. Y. and Saigal, S., "A Curved Quadrilateral Element for Static Analysis of Shells with Geometric and Material Nonlinearities," *International Journal for Numerical Methods in Engineering,* Vol. 21, April 1985, pp. 617–635.

[40]Bushnell, D., "Computerized Analysis of Shells—Governing Equations," *Computers and Structures,* Vol. 18, March 1984, pp. 471–536.

[41]Khojasteh-Bakht, M., "Analysis of Elastic-Plastic Shells of Revolution Under Axisymmetric Loading by the Finite Element Method," Ph.D. Dissertation, Dept. of Civil Engineering, Univ. of California—Berkeley, Berkeley, CA, 1967.

[42]Zienkiewicz, O. C. and Nayak, G. C., "A General Approach to Problems of Plasticity and Large Deflection Using Isoparametric Elements," *Proceedings of the Conference on Matrix Methods in Structural Mechanics,* Wright-Patterson AFB, Ohio, 1971, pp. 881–928.

[43]Surana, K. S., "Geometrically Nonlinear Formulation for the Axisymmetric Shell Elements," *International Journal for Numerical Methods in Engineering,* Vol. 18, April 1982, pp. 477–502.

[44]Moore, C. J., Yang, T. Y., and Anderson, D. C., "A New 48 D.O.F. Quadrilateral Shell Element with Variable Order Polynomial and Rational B-Spline Geometries with Rigid Body Modes," *International Journal for Numerical Methods in Engineering,* Vol. 20, Nov. 1984, pp. 2121–2142.

[45]Argyris, J. H., Balmer, H., Kleiber, M., and Hindenlang, U., "Natural Description of Large Inelastic Deformations for Shells of Arbitrary Shape—Application of TRUMP Element," *Computer Methods in Applied Mechanics and Engineering,* Vol. 22, March 1980, pp. 361–389.

[46]Parisch, H., "Large Displacements of Shells Including Material Nonlinearities," *Computer Methods in Applied Mechanics and Engineering,* Vol. 27, Feb. 1981, pp. 183–214.

[47]Argyris, J. H. and Scharpf, D. W., "The SHEBA Family of Shell Elements for the Matrix Displacement Method," *The Aeronautical Journal of the Royal Aeronautical Society,* Vol. 72, 1968, pp. 873–883.

[48]Sabir, A. B. and Lock, A. C., "The Application of Finite Elements to the Large Deflection Geometrically Nonlinear Behavior of Cylindrical Shells," *Variational Methods in Engineering,* edited by W. A. Brebbia and H. Tottenham, Southampton Univ. Press, Southampton, England, UK, 1972, pp. 7/66–7/75.

[49]Ramm, E., "Strategies for Tracing the Nonlinear Response Near Limit Points," *Nonlinear Elastic Analysis in Structural Mechanics,* edited by W. Wunderlich, E. Stein, and K. J. Bathe, Proceedings of the Europe-U.S. Workshop, Ruhr-Universität Bochum, Springer-Verlag, Berlin, 1980.

[50]Wempner, G. A., "Discrete Approximations Related to Nonlinear Theories of Solids," *International Journal of Solids and Structures,* Vol. 7, Oct. 1971, pp. 1581–1599.

[51]Riks, E., "An Incremental Approach to the Solution of Snapping and Buckling Problems," *International Journal of Solids and Structures,* Vol. 15, April 1979, pp. 529–551.

[52]Bergan, P. G., "Solution Algorithms for Nonlinear Problems," *Computers and Structures,* Vol. 12, No. 4, Oct. 1980, pp. 497–509.

[53]Batoz, J.-L. and Dhatt, G., "Incremental Displacement Algorithms for Nonlinear Problems," *International Journal for Numerical Methods in Engineering,* Vol. 14, Aug. 1979, pp. 1262–1267.